

A model reduction method based on nonlinear optimization for multiscale stochastic optimal control problems

Jingyi Zhang

October 14, 2025

Abstract

This paper presents a nonlinear optimization-based model reduction method for multiscale stochastic optimal control problems governed by stochastic partial differential equations. The proposed approach constructs a non-intrusive, data-driven reduced-order model by employing a parameter-separable structure to handle stochastic dependencies and directly minimizing the \mathcal{L}^2 norm of the output error via gradient-based optimization. Compared to existing methods, this framework offers three significant advantages: it is entirely data-driven, relying solely on output measurements without requiring access to internal system matrices; it guarantees approximation accuracy for control outputs, aligning directly with the optimization objective; and its computational complexity is independent of the original PDE dimension, ensuring feasibility for real-time control applications. Numerical experiments on stochastic diffusion and advection-diffusion equations demonstrate the method's effectiveness and efficiency, providing a systematic solution for the real-time control of complex uncertain systems and bridging the gap between model reduction theory and practical engineering.

1 Introduction

Optimal control problems play a crucial role in various fields of science and engineering, where the goal is to determine the optimal control strategy that minimizes or maximizes a given objective function while satisfying certain constraints. When modeling physical processes with partial differential equations (PDEs), these problems often involve complex interactions between the control inputs and the underlying dynamics of the system. However, in real-world applications, uncertainties are inevitably present in the system parameters, boundary conditions, external loadings, or even the shape of the physical domain. These uncertainties can significantly impact the performance of the optimal control strategy, making it essential to incorporate stochastic information into the control problem formulation.

In recent years, stochastic optimal control problems governed by stochastic PDEs have attracted increasing attention due to their ability to account for uncertainties in a rigorous and systematic manner. By introducing random variables to parameterize the stochastic functions, these problems provide a more realistic framework for modeling

and optimizing control strategies under uncertain conditions. For deterministic optimal control problems, extensive research has been conducted over the past decades, resulting in well-developed mathematical theories and efficient computational methods [1–3]. In contrast, the development of stochastic optimal control problems, especially those involving stochastic PDEs, has only gained substantial progress in the last few decades [4–8]. Despite these advancements, there remain significant challenges in both the theoretical and computational aspects of stochastic optimal control, particularly in handling high-dimensional uncertainties and developing efficient numerical algorithms.

In this study, we focus on stochastic optimal control problems with a quadratic cost functional that are subject to constraints imposed by stochastic partial differential equations. Within the realm of PDE-constrained optimization, there exists a fundamental decision point: whether to adopt a discretize-then-optimize approach or an optimize-then-discretize approach. The literature presents divergent views on the merits of each strategy [9]. After careful consideration, we have elected to pursue the optimize-then-discretize methodology in the present paper. In solving stochastic optimal control problems, particularly those involving PDE-constrained optimization, a range of significant challenges arise. Firstly, the computational cost of high-dimensional integration increases exponentially with the dimensionality, leading to the "curse of dimensionality." Secondly, solving PDE-constrained optimization problems requires solving multiple partial differential equations simultaneously, including the state equation, the adjoint equation, and a set of equations ensuring the optimality of the solution, making the computational process very time-consuming and complex. Furthermore, in the context of many queries for parameterized PDEs, the need to solve for multiple parameter values significantly increases the computational load, especially when the parameter space is large or infinite. Finally, in high-dimensional stochastic spaces, the exponential growth of computational complexity makes numerical computation extremely difficult and time-consuming. These challenges necessitate the selection and development of efficient numerical methods, such as reduced-order models, adaptive mesh methods, or parallel computing techniques, to improve computational efficiency and the feasibility of practical applications.

Model reduction methods have become indispensable tools for tackling high-dimensional control problems governed by PDEs. Classical approaches such as Proper Orthogonal Decomposition (POD) and Galerkin projection construct reduced-order models (ROMs) by projecting the full-order system onto carefully chosen subspaces. While these methods have achieved success in deterministic scenarios, they exhibit significant limitations when dealing with stochastic optimal control problems: First, such methods typically require direct manipulation of the full order model's system matrices. Second, when handling high-dimensional stochastic parameter spaces, the combination of traditional Monte Carlo sampling and POD faces the challenge of the "curse of dimensionality." Finally, existing methods mainly focus on the approximation accuracy of state variables while neglecting the optimization of output errors directly related to control objectives.

In order to address the above issues, this paper presents a non-intrusive \mathcal{L}^2 -optimal model order reduction approach for stochastic optimal control problems. The method innovatively employs a parameter-separable form to handle the dependence on stochastic parameters, and directly minimizes the \mathcal{L}^2 norm of output errors through gradient optimization techniques. Compared with existing methods, this approach has three significant advantages: Firstly, it is completely data-driven based on output measurements,

eliminating the need to access the internal system matrices. Secondly, it guarantees the approximation accuracy of control outputs, directly aligning with the optimization of control objectives. In addition, its computational complexity is independent of the original PDE dimensionality, ensuring feasibility for real-time control applications.

The structure of this paper is arranged as follows: Section 2 presents the relevant definitions of stochastic optimal control problems, Section 3 elaborates on the construction of the \mathcal{L}^2 -optimal reduced-order model for stochastic optimal control problems in detail, Section 4 introduces the generalized multiscale finite element method, Section 5 verifies the effectiveness of the method in stochastic coefficient PDE-constrained problems through numerical experiments, and this approach provides a systematic solution for real-time control of complex uncertain systems, bridging the gap between model order reduction theory and practical engineering applications.

2 Preliminaries

This paper mainly applies a data-driven, nonlinear optimization method to the stochastic control problem controlled by partial differential equations. In this section, the stochastic control problem is briefly introduced and approximated by the finite element method so that we can obtain the discrete form of the model.

2.1 Stochastic optimal control problem

Let $(\mathcal{D}, \mathcal{F})$ be a measurable space where \mathcal{D} is the set of possible outcomes $\omega \in \mathcal{D}$ and $\mathcal{F} \subset 2^{\mathcal{D}}$ is a σ -algebra of events. We denote the expected value of a random variable $X : \mathcal{D} \rightarrow \mathbb{R}$ with respect to a probability measure $\mathcal{P} : \mathcal{F} \rightarrow [0, 1]$ defined on the measurable space $(\mathcal{D}, \mathcal{F})$ by

$$\mathbb{E}_{\mathcal{P}}[X] = \int_{\mathcal{D}} X(\omega) d\mathcal{P}(\omega).$$

We denote the usual Lebesgue space of $r \in [1, \infty)$ integrable real-valued functions by

$$L^r(\mathcal{D}, \mathcal{F}, \mathcal{P}) := \{\theta : \mathcal{D} \rightarrow \mathbb{R} : \theta \text{ is } \mathcal{F}\text{-measurable, } \mathbb{E}_{\mathcal{P}}[|\theta|^r] < \infty\}.$$

The Lebesgue spaces defined on $(\mathcal{D}, \mathcal{F}, \mathcal{P})$ are Banach spaces and serve as natural spaces for real-valued random variables, i.e., \mathcal{F} -measurable functions.

We assume that Ω is a convex bounded polygonal domain in $\mathbb{R}^d (d \geq 1)$ with Lipschitz continuous boundary $\partial\Omega$. Given a real Hilbert space $H^s(\Omega)$, the tensor-product vector space associated with $L^2(\mathcal{D}, \mathcal{F}, \mathcal{P})$ and $H^s(\Omega)$ is

$$L^2(\mathcal{D}, \mathcal{F}, \mathcal{P}) \otimes H^s(\Omega) := \text{span} \{\theta v : \theta \in L^2(\mathcal{D}, \mathcal{F}, \mathcal{P}), v \in H^s(\Omega)\}.$$

We denote $\mathcal{H}^s(\Omega) := L^2(\mathcal{D}, \mathcal{F}, \mathcal{P}) \otimes H^s(\Omega)$ to shorten the notation and equip it with the following norm

$$\|u\|_{\mathcal{H}^s(\Omega)} = \mathbb{E}_{\mathcal{P}}[\|u\|_{H^s}^2]^{\frac{1}{2}}.$$

In particular, $\mathcal{H}_0^s(\Omega) = \{u \in \mathcal{H}^s(\Omega) : u|_{\partial\Omega} = 0\}$. When $s = 0$, we employ the abbreviated notion $\mathcal{L}^2(\Omega)$ to denote $\mathcal{H}^0(\Omega)$ by convention.

The stochastic optimal control problem is to minimize the objective functional under some constraints, which is mainly divided into distributed control problems and boundary control problems. The main research object of this paper is the former, and now we give the form of the stochastic distributed control problem. The objective functional is

$$\min_{\substack{u \in \mathcal{H}^1(\Omega) \\ f \in \mathcal{L}^2(\Omega)}} J(u, f) := \frac{1}{2} \|u(x, \mu(\omega)) - \hat{u}(x, \mu(\omega))\|_{\mathcal{L}^2(\Omega)}^2 + \beta \|f(x, \mu(\omega))\|_{\mathcal{L}^2(\Omega)}^2 \quad (2.1)$$

which is constrained by a stochastic PDE with the following variational form

$$a(u, v; \mu(\omega)) = (f, v; \mu(\omega)), \forall v \in \mathcal{H}_0^1(\Omega), \quad (2.2)$$

subject to the Dirichlet boundary condition $u|_{\partial\Omega} = g(x)$. Here, $J(u, f) : \Omega \times \mathcal{D} \rightarrow \mathbb{R}$ is the cost functional.

In the model problem, we assume that the control function $f(x, \mu(\omega))$ and the state function $u(x, \mu(\omega))$ are random fields represented by a random vector μ . The objective of the stochastic control problem is to select a suitable $f(x, \mu(\omega))$ so that the corresponding $u(x, \mu(\omega))$ is the best possible approximation of the expected $\hat{u}(x, \mu(\omega))$.

Because the problem is poorly posed, the second term, namely the Tikhonov regularization term, is added to the cost functional (2.1). It is necessary to determine the Tikhonov parameter β . Although it is generally selected a priori, a value around $\beta = 10^{-2}$ is commonly used.

Finally, according to (2.1), (2.2) and the boundary condition, we write the stochastic control problem in the following form:

$$\begin{cases} \min_{\substack{u \in \mathcal{H}^1(\Omega) \\ f \in \mathcal{L}^2(\Omega)}} J(u, f) = \frac{1}{2} \|u - \hat{u}\|_{\mathcal{L}^2(\Omega)}^2 + \beta \|f\|_{\mathcal{L}^2(\Omega)}^2, \\ \text{s.t. } a(u, v; \mu(\omega)) = (f, v; \mu(\omega)), \forall v \in \mathcal{H}_0^1(\Omega), \text{ in } \Omega \\ \quad u = g(x), \text{ on } \partial\Omega. \end{cases} \quad (2.3)$$

2.2 Formulation and structure.

In order to solve (2.3) numerically, generally speaking, there are two different methods, the first one is discretize-then-optimize, and the second one is optimize-then-discretize. In some cases, these two methods will produce the same numerical results. However, from a structural point of view, they are different. This subsection discusses the second method in detail.

Firstly, we derive the stochastic optimality system of the optimal control problem by using Lagrangian approach, and then give the framework of FE approximation for stochastic optimal control problems.

We define the following stochastic Lagrangian functional as

$$\mathcal{L}(u, f, \lambda) := J(u, f) + a(u, \lambda; \mu) - (f, \lambda; \mu), \quad (2.4)$$

where $\lambda \in \mathcal{H}_0^1(\Omega)$ is the Lagrangian parameter or adjoint variable. By taking the Fréchet derivative of Lagrangian functional (2.4) for the variables λ , u and f , and

evaluating them at \tilde{u} , \tilde{f} and $\tilde{\lambda}$. We can obtain the first-order necessary optimality conditions of stochastic control problems (2.3)

$$\begin{cases} a(u, \tilde{u}; \mu) = (f, \tilde{u}; \mu), \forall \tilde{u} \in \mathcal{H}_0^1(\Omega), \\ a'(\lambda, \tilde{\lambda}; \mu) = -(u - \hat{u}, \tilde{\lambda}; \mu), \forall \tilde{\lambda} \in \mathcal{H}_0^1(\Omega), \\ 2\beta(f, \tilde{f}; \mu) = (\tilde{f}, \lambda; \mu), \forall \tilde{f} \in \mathcal{L}^2(\Omega), \end{cases} \quad (2.5)$$

where $(\cdot, \cdot; \mu)$ represents the general inner product L^2 and $a'(\lambda, \tilde{\lambda}; \mu) = a(\tilde{\lambda}, \lambda; \mu)$ is the adjoint bilinear form. These three equations are, respectively, the state equation, adjoint equation and gradient equation.

The optimality system (2.5) only has local optimal solutions, in order to prove the global existence and uniqueness of the optimal solution, we need to derive the stochastic saddle point formula of the optimal control problem (2.3).

We introduce some new definitions at first so that we have a minimization problem equivalent to the original optimal problem (2.3). Let $\underline{u} = (u, f) \in \mathcal{U}$ and $\underline{v} = (v, h) \in \mathcal{U}$, here the tensor space $\mathcal{U} = \mathcal{H}^1(\Omega) \times \mathcal{L}^2(\Omega)$ equipped with the norm $\|\underline{u}\|_{\mathcal{U}} = \|u\|_{\mathcal{H}^1(\Omega)} + \|f\|_{\mathcal{L}^2(\Omega)}$. We also define bilinear forms

$$\begin{cases} \mathcal{A}(\underline{u}, \underline{v}) := (u, v) + 2\beta(f, h; \mu), \\ \mathcal{B}(\underline{u}, q) := a(u, q; \mu) - (f, q; \mu), \end{cases} \quad (2.6)$$

where $\mathcal{A}(\cdot, \cdot) : \mathcal{U} \times \mathcal{U} \rightarrow \mathbb{R}$ and $\mathcal{B}(\cdot, \cdot) : \mathcal{U} \times \mathcal{H}_0^1(\Omega) \rightarrow \mathbb{R}$. Giving $\hat{u} = (\hat{u}, 0)$, $(\hat{u}, \underline{u}) = (\hat{u}, u)$ and $\mathcal{U}_{ad} \subset \mathcal{U}$, the equivalent form is

$$\begin{cases} \min_{\underline{u} \in \mathcal{U}_{ad}} \mathcal{J}(\underline{u}) = \frac{1}{2} \mathcal{A}(\underline{u}, \underline{u}) - (\hat{u}, \underline{u}), \\ \text{s.t. } \mathcal{B}(\underline{u}, \tilde{u}) = (g, \tilde{u})_{\partial\Omega}, \forall \tilde{u} \in \mathcal{H}_0^1(\Omega). \end{cases} \quad (2.7)$$

Moreover, combining (2.5) with (2.6), the equivalent saddle point problem for (2.7) is to find $(\underline{u}, \lambda) \in \mathcal{U} \times \mathcal{H}_0^1(\Omega)$ such that

$$\begin{cases} \mathcal{A}(\underline{u}, \underline{v}) + \mathcal{B}(\underline{v}, \lambda) = (\hat{u}, \underline{v}), \quad \forall \underline{v} \in \mathcal{U}, \\ \mathcal{B}(\underline{u}, \tilde{u}) = (g, \tilde{u})_{\partial\Omega}, \quad \forall \tilde{u} \in \mathcal{H}_0^1(\Omega). \end{cases} \quad (2.8)$$

Please refer to [] for the equivalent relationship between the saddle point form of stochastic control problem and other forms, and we will not repeat it here.

Theorem 2.1. *Let $\mathcal{U}_0 := \{\underline{u} \in \mathcal{U} : \mathcal{B}(\underline{u}, \tilde{u}) = 0, \forall \tilde{u} \in \mathcal{H}_0^1(\Omega)\}$ be the kernel space of bilinear form $\mathcal{B}(\cdot, \cdot)$, we can obtain the global existence of a unique solution to the minimization problem (2.8).*

The above is to optimize the stochastic control problem (2.3) and get the saddle point formation, and then discretize it with finite element approximation.

Let \mathcal{T}_h be a uniform partition of the domain Ω , N_h be the number of vertices, N_e be the number of elements in the fine mesh \mathcal{T}_h and the dimension of FE space be \mathcal{N} . The FE space defined on the fine mesh is $V^h(\Omega) \subset H^1(\Omega)$, and $V_0^h(\Omega) \subset V^h(\Omega)$ has the vanishing boundary values. Furthermore, we define $\mathcal{V}_0^h(\Omega) := V_0^h(\Omega) \otimes L^2(\Gamma)$ and

$\mathcal{M}_h(\Omega) := M_h(\Omega) \otimes L^2(\Gamma)$ which $M_h(\Omega)$ is the finite dimensional subspace of $L^2(\Omega)$, so $\mathcal{M}_h(\Omega)$ is also the finite dimensional subspace of $\mathcal{L}^2(\Omega)$.

Giving any $\mu \in \Gamma$, applying the Galerkin projection of $\mathcal{U}_h \times \mathcal{V}_0^h(\Omega) \subset \mathcal{U} \times \mathcal{H}_0^1(\Omega)$, where $\mathcal{U}_h := \mathcal{V}_0^h(\Omega) \times \mathcal{M}_h(\Omega)$, we can get the FEM discrete formation of saddle point problem (2.8): find $(\underline{u}_h, \lambda_h) \in \mathcal{U}_h \times \mathcal{V}_0^h$ s.t.

$$\begin{cases} \mathcal{A}(\underline{u}_h, \underline{v}_h) + \mathcal{B}(\underline{v}_h, \lambda_h) = (\hat{u}, \underline{v}_h), & \forall \underline{v}_h \in \mathcal{U}_h, \\ \mathcal{B}(\underline{u}_h, \tilde{u}_h) = (g, \tilde{u}_h)_{\partial\Omega}, & \forall \tilde{u}_h \in \mathcal{V}_0^h(\Omega). \end{cases} \quad (2.9)$$

The Galerkin formulation of (2.5) is to find $(u_h, f_h, \lambda_h) \in \mathcal{V}_0^h(\Omega) \times \mathcal{M}_h(\Omega) \times \mathcal{V}_0^h$, such that

$$\begin{cases} a(u_h, \tilde{u}_h; \mu) = (f_h, \tilde{u}_h; \mu), & \forall \tilde{u}_h \in \mathcal{V}_0^h(\Omega), \\ a(\lambda_h, \tilde{\lambda}_h; \mu) = -(u_h - \hat{u}, \tilde{\lambda}_h; \mu), & \forall \tilde{\lambda}_h \in \mathcal{V}_0^h(\Omega), \\ 2\beta(f_h, \tilde{f}_h; \mu) = (\tilde{f}_h, \lambda_h; \mu), & \forall \tilde{f}_h \in \mathcal{M}_h(\Omega). \end{cases} \quad (2.10)$$

Assuming that the basis functions of the spaces $\mathcal{M}_h(\Omega)$ and $\mathcal{V}_0^h(\Omega)$ are represented by $\{\phi_k\}_{k=1}^{N_e}$ and $\{\psi_k\}_{k=1}^{N_e}$, then we can express the variables u_h, f_h, λ_h in (2.10) by the linear combination of the corresponding basis functions

$$u_h = \sum_{i=1}^{N_h} u_{h,i} \psi_i, \quad f_h = \sum_{j=1}^{N_e} f_{h,j} \phi_j, \quad \lambda_h = \sum_{k=1}^{N_h} \lambda_{h,k} \psi_k. \quad (2.11)$$

For the weak form (2.2), we will make an assumption that the parameter bilinear form $a(\cdot, \cdot; \mu)$ and the parameter linear form $(f, \cdot; \mu)$ is affine with respect to μ , that is,

$$\begin{cases} a(u, v; \mu) = \sum_{q=1}^{Q_a} Q_a^q(\mu) a^q(u, v) & \forall u, v \in H^1(\Omega), \forall \mu \in \Gamma, \\ (f, v; \mu) = \sum_{q=1}^{Q_f} Q_f^q(\mu) (f^q, v) & \forall f^q \in L^2(\Omega), v \in H^1(\Omega), \forall \mu \in \Gamma, \end{cases} \quad (2.12)$$

where $Q_a^q(\mu) : \Gamma \rightarrow \mathbb{R}$ and $Q_f^q(\mu) : \Gamma \rightarrow \mathbb{R}$ are μ -dependent function, in addition, $a_q(\cdot, \cdot) : H^1(\Omega) \times H^1(\Omega) \rightarrow \mathbb{R}$ and $(f^q, \cdot) : L^2(\Omega) \times H^1(\Omega) \rightarrow \mathbb{R}$ are independent of μ .

If the $a(\cdot, \cdot; \mu)$ and $(f, \cdot; \mu)$ in (2.10) are affine with respect to μ , satisfying (2.12), and with the (2.11), the discrete optimality system (2.10) can be

$$\begin{cases} \sum_{q=1}^{Q_a} \sum_{i=1}^{N_h} Q_a^q(\mu) u_{h,i}(\mu) a^q(\psi_i, \psi_{i'}) = \sum_{j=1}^{N_e} f_{h,j}(\mu) (\phi_j, \psi_{i'}), \\ \sum_{q'=1}^{Q_a} \sum_{k=1}^{N_h} Q_a^{q'}(\mu) \lambda_{h,k}(\mu) a^{q'}(\psi_k, \psi_{k'}) + \sum_{i=1}^{N_h} u_{h,i}(\mu) (\psi_i, \psi_{k'}) = \sum_{p=1}^{Q_u} \hat{u}_p(\mu) (\bar{u}_p, \psi_{k'}), \\ 2\beta \sum_{j=1}^{N_e} f_{h,j}(\mu) (\phi_j, \phi_{j'}) = \sum_{k=1}^{N_h} \lambda_{h,k}(\mu) (\phi_{j'}, \psi_k). \end{cases}$$

In order to convert the above formula into matrix-vector form, we first assume that

$$\begin{aligned}
(M_1)_{j,j'} &= (\phi_j, \phi_{j'}), 1 \leq j, j' \leq N_e, \\
(M_2)_{k,j'} &= (\phi_{j'}, \psi_k), 1 \leq j' \leq N_e, 1 \leq k \leq N_h, \\
(M_3)_{i,k'} &= (\psi_i, \psi_{k'}), 1 \leq i, k, k' \leq N_h, \\
(K^q)_{k,k'} &= a^q (\psi_k, \psi_{k'}), 1 \leq i, k, k' \leq N_h, \\
\left(\widehat{U}_p\right)_{k'} &= (\widehat{u}_p, \psi_{k'}), 1 \leq k, k' \leq N_h, \\
K &= \sum_{q=1}^{Q_a} Q_a^q(\mu) K^q, \quad \widehat{U} = \sum_{p=1}^{Q_u} \widehat{u}_p(\mu) \widehat{U}_p.
\end{aligned}$$

here $\{K^q\}_{q=1}^{Q_a}$ are stiffness matrices, $\{M_i\}_{i=1}^3$ are mass matrices, and $\{\widehat{U}_p\}_{p=1}^{Q_u}$ are load vectors. Then, we can get the algebraic formulation of (2.10),

$$\underbrace{\begin{bmatrix} 2\beta M_1 & 0 & -M_2^T \\ 0 & M_3 & K^T(\mu) \\ -M_2 & K(\mu) & 0 \end{bmatrix}}_{\mathcal{A}_h(\mu) \in \mathbb{R}^{(2N_h+N_e) \times (2N_h+N_e)}} \begin{bmatrix} F(\mu) \\ U(\mu) \\ \Lambda(\mu) \end{bmatrix} = \begin{bmatrix} 0 \\ \widehat{U}(\mu) \\ d \end{bmatrix}, \quad (2.13)$$

where $U(\mu)$, $F(\mu)$ and $\Lambda(\mu)$ denote the vectors of the coefficients in the expansion of $u_h(\mu)$, $f_h(\mu)$ and $\lambda_h(\mu)$ and the term coming from the boundary values of u_h is denoted by d .

3 \mathcal{L}_2 -optimal reduced-order modeling

In this section, we give a non-invasive, data-driven, gradient-based descent algorithm to solve the stochastic control problem (2.13), aiming at optimization problem with parameter-separable forms, this method only uses output samples to construct the optimal approximant.

3.1 The establishment of the model

Given a distributed stochastic control problem in the form of (2.3), we can transform it into the algebraic formulation of (2.13) first optimizing and then discretizing it. We define $x(\mu) := [F(\mu), U(\mu), \Lambda(\mu)]^T$ in the (2.13) as the state quantity, we consider the following problem: giving $\mu \in \Gamma$, evaluate

$$y(\mu) = \ell(x(\mu)), \quad (3.1)$$

and $x(\mu)$ satisfy

$$\begin{bmatrix} 2\beta M_1 & 0 & -M_2^T \\ 0 & M_3 & K^T(\mu) \\ -M & K(\mu) & 0 \end{bmatrix} x(\mu) = \begin{bmatrix} 0 \\ \widehat{U}(\mu) \\ d \end{bmatrix}, \quad (3.2)$$

where ℓ is a bounded linear functional, $x(\mu) \in \mathbb{R}^{(2N_h+N_e) \times 1}$ is the state, $y(\mu) \in \mathbb{R}$ is the output. By introducing a matrix $C(\mu) \in \mathbb{R}^{1 \times (2N_h+N_e)}$, the problem function (3.1) is discretized into

$$y(\mu) = C(\mu)x(\mu). \quad (3.3)$$

We emphasize that our ultimate interest is the output prediction $y(\mu)$: the state variable $x(\mu)$ serves as an intermediary. We call the above model in (3.2) and (3.3) the full-order model (FOM). In addition, we can rewrite the above model into a direct approximation/interpolation of the input-output mapping

$$y : \Gamma \rightarrow \mathbb{R}, \quad \mu \mapsto y(\mu). \quad (3.4)$$

Since the full-order matrices $M_1, M_2, M_3, K(\mu), \bar{U}(\mu)$ and $C(\mu)$ are must be accessed, so that it is very expensive to calculate $y(\mu)$ for a given μ in FOM. What we are interested in is that how to calculate $y(\mu)$ without accessing to the above internal representations.

As mentioned in section 2.2, we assume that we are given FE approximation spaces $V^h(\Omega)$ and $M_h(\Omega)$ of dimension \mathcal{N} and N_e in the fine grid \mathcal{T}_h . We define the spaces of the state, control and adjoint variables as $X_h^{\mathcal{N}}(\Omega), Y_h^{\mathcal{N}}(\Omega)$ and $Z_h^{\mathcal{N}}(\Omega)$. We then introduce, given a positive integer N_{max} , an associated sequence of approximation spaces: for $N = 1, \dots, N_{max}$, $X_h^N(\Omega)$ is a N -dimensional subspace of $X_h^{\mathcal{N}}(\Omega)$; we further suppose that $X_h^1(\Omega) \subset X_h^2(\Omega) \subset \dots \subset X_h^{N_{max}}(\Omega) \subset X_h^{\mathcal{N}}(\Omega)$. Similarly, for the control variable f and adjoint variable λ , we have $Y_h^1(\Omega) \subset Y_h^2(\Omega) \subset \dots \subset Y_h^{N_{max}}(\Omega) \subset Y_h^{\mathcal{N}}(\Omega)$ and $Z_h^1(\Omega) \subset Z_h^2(\Omega) \subset \dots \subset Z_h^{N_{max}}(\Omega) \subset Z_h^{\mathcal{N}}(\Omega)$.

By using Galerkin projection onto the low-dimensional subspace $X_h^N(\Omega) \times Y_h^N(\Omega) \times Z_h^N(\Omega)$, the associated optimality system is: given $\mu \in \Gamma$, find $(u_h^N, f_h^N, \lambda_h^N) \in X_h^N(\Omega) \times Y_h^N(\Omega) \times Z_h^N(\Omega)$ such that

$$\begin{cases} a(u_h^N, \tilde{u}_h'; \mu) = (f_h^N, \tilde{u}_h'; \mu), \quad \forall \tilde{u}_h' \in X_h^N(\Omega), \\ a(\lambda_h^N, \tilde{\lambda}_h'; \mu) = -(u_h^N - \hat{u}, \tilde{\lambda}_h'; \mu), \quad \forall \tilde{\lambda}_h' \in Z_h^N(\Omega), \\ 2\beta(f_h^N, \tilde{f}_h'; \mu) = (\tilde{f}_h', \lambda_h^N; \mu), \quad \forall \tilde{f}_h' \in Y_h^N(\Omega). \end{cases} \quad (3.5)$$

We then choose the sets $\{\delta_i\}_{i=1}^{2N}$ as our basis for $X_h^N(\Omega)$ and $Z_h^N(\Omega)$, $\{\xi_j\}_{j=1}^N$ as basis for $Y_h^N(\Omega)$. Because basis function δ_i and ξ_j belong to the FEM space $V_0^h(\Omega)$ and $M_h(\Omega)$, they can be written as

$$\begin{aligned} \delta_i &= \sum_{k=1}^{N_h} W_{i,k} \psi_k, \quad i = 1, \dots, 2N, \\ \xi_j &= \sum_{s=1}^{N_e} V_{j,s} \phi_s, \quad j = 1, \dots, N. \end{aligned}$$

Similar to the derivation process in Section 2.2, the matrix form of (3.5) is as follows

$$\begin{cases} \sum_{q=1}^{Q_a} Q_a^q(\mu) (W^T K^q W) U_g(\mu) = W^T M_2^T V F_g(\mu), \\ \sum_{q'=1}^{Q_a} Q_a^{q'}(\mu) (W^T K^{q'} W) \Lambda_g(\mu) + W^T M_3 W U_g(\mu) = \sum_{p=1}^{Q_u} \hat{u}_p(\mu) (W^T \bar{U}_p), \\ 2\beta V^T M_1 V^T F_g(\mu) = V^T M_2 W \Lambda_g(\mu), \end{cases} \quad (3.6)$$

With the following notations,

$$\begin{aligned} K_g(\mu) &= \sum_{q=1}^{Q_a} Q_a^q(\mu)(W^T K^q W), \\ \widehat{U}_g &= \sum_{p=1}^{Q_u} \widehat{u}_p(\mu)(W^T \widehat{U}_p), \\ M_{1,g} &= V^T M_1 V, M_{2,g} = W^T M_2 V, M_{3,g} = W^T M_1 W, \end{aligned}$$

we can get the algebraic formulation of (3.5)

$$\underbrace{\begin{bmatrix} 2\beta M_{1,g} & 0 & -M_{2,g}^T \\ 0 & M_{3,g} & K_g^T(\mu) \\ -M_{2,g} & K_g(\mu) & 0 \end{bmatrix}}_{\mathcal{A}_g(\mu) \in \mathbb{R}^{5N \times 5N}} \begin{bmatrix} F_g(\mu) \\ U_g(\mu) \\ \Lambda_g(\mu) \end{bmatrix} = \begin{bmatrix} 0 \\ \widehat{U}_g(\mu) \\ d_g \end{bmatrix}. \quad (3.7)$$

The dimension of this linear system is obviously lower than that of (3.2).

We define $\widehat{x}(\mu) := [F_g(\mu), U_g(\mu), \Lambda_g(\mu)]^T$, obviously, the state-interest function (3.3) rewrites as

$$\widehat{y}(\mu) = C(\mu) \begin{bmatrix} V^T & 0 & 0 \\ 0 & W^T & 0 \\ 0 & 0 & W^T \end{bmatrix} \widehat{x}(\mu) := C_g(\mu) \widehat{x}(\mu), \quad (3.8)$$

and then we have the input-output mapping of the system (3.7)

$$\widehat{y} : \Gamma \rightarrow \mathbb{R}, \quad \mu \mapsto \widehat{y}(\mu). \quad (3.9)$$

Now we obtain the reduced-order model (ROM) (3.7) and (3.8), comparing the FOM and the ROM, N is a modest integer so that evaluating $\widehat{y}(\mu)$ is cheaper than evaluating $y(\mu)$, and $\widehat{y}(\mu)$ is close to $y(\mu)$ for all $\mu \in \Gamma$.

Our goal is to construct a data-driven reduced-order model (DDROM)

$$\underbrace{\begin{bmatrix} 2\beta M_{1,r} & 0 & -M_{2,r}^T \\ 0 & M_{3,r} & K_r^T(\mu) \\ -M_{2,r} & K_r(\mu) & 0 \end{bmatrix}}_{\mathcal{A}_r(\mu) \in \mathbb{R}^{r \times r}} \widehat{x}(\mu) = \begin{bmatrix} 0 \\ \widehat{U}_r(\mu) \\ d_r \end{bmatrix}, \quad (3.10)$$

and

$$\widehat{y}(\mu) = C_r(\mu) \widehat{x}(\mu), \quad (3.11)$$

whose output $\widehat{y}(\mu)$ is significantly cheaper to evaluate compared to $y(\mu)$, and $\widehat{y}(\mu)$ is close to $\widehat{y}(\mu)$ for all $\mu \in \Gamma$. Although the motivation comes from FOM of the form in (3.2) and (3.3), the approximation framework we develop below only requires access to the parameter-to-output mapping (3.4) and not to the full-order matrices and state x in the FOM. Thus, the work with a nonintrusive parameter/output data-driven formulation.

As for measuring the distance between y and \widehat{y} to find a DDROM, the \mathcal{L}_2 -optimal reduced-order modeling introduced in this section minimizes the \mathcal{L}_2 error

$$\|y - \widehat{y}\|_{\mathcal{L}_2} = \left(\int_{\Gamma} \|y(\mu) - \widehat{y}(\mu)\|_{\mathcal{F}}^2 d\mu \right)^{1/2}, \quad (3.12)$$

where the $\|\cdot\|_{\mathcal{F}}$ is the Frobenius norm. All in all, given the input-to-output mapping in (3.4), our goal is to find a DDROM consisting of (3.10) and (3.11) that minimizes the output \mathcal{L}_2 error (3.12).

3.2 Optimization problem with parameter-separable forms

In section 2.2, we assume that the parameter bilinear form $a(\cdot, \cdot; \mu)$ and the parameter linear form $(f, \cdot; \mu)$ is affine with respect to μ , as described in (2.12). In addition, make a similar affine assumption for the functional $(\ell, x; \mu)$ in (3.1),

$$(\ell, x; \mu) = \sum_{k=1}^{Q_l} Q_l^k(\mu)(\ell^k, x), \quad \forall \ell^k \in L^2(\Omega), x \in \mathbb{R}^{(2N_h+N_e) \times 1}, \forall \mu \in \Gamma. \quad (3.13)$$

Then we can rewrite the FOM system (3.2) and (3.3) as a parameter-separable form

$$\begin{aligned} & \left\{ \begin{bmatrix} 2\beta M_1 & 0 & -M_2^T \\ 0 & M_3 & 0 \\ -M_2 & 0 & 0 \end{bmatrix} + \sum_{q=1}^{Q_a} Q_a^q(\mu) \begin{bmatrix} 0 & 0 & 0 \\ 0 & 0 & (K^q)^T \\ 0 & K^q & 0 \end{bmatrix} \right\} x(\mu) \\ &= \begin{bmatrix} 0 \\ 0 \\ d \end{bmatrix} + \sum_{p=1}^{Q_u} \hat{u}_p(\mu) \begin{bmatrix} 0 \\ \hat{U}_p \\ 0 \end{bmatrix}, \end{aligned} \quad (3.14)$$

and

$$y(\mu) = \sum_{k=1}^{Q_l} Q_l^k(\mu) C_k x(\mu). \quad (3.15)$$

This form is preserved in the classical Galerkin projection ROM (3.7),

$$\begin{aligned} & \left\{ \begin{bmatrix} 2\beta V^T M_1 V & 0 & -V^T M_2^T W \\ 0 & W^T M_3 W & 0 \\ -W^T M_2 V & 0 & 0 \end{bmatrix} + \sum_{q=1}^{Q_a} Q_a^q(\mu) \begin{bmatrix} 0 & 0 & 0 \\ 0 & 0 & W^T (K^q)^T W \\ 0 & W^T K^q W & 0 \end{bmatrix} \right\} \hat{x}(\mu) \\ &= \begin{bmatrix} 0 \\ 0 \\ d_g \end{bmatrix} + \sum_{p=1}^{Q_u} \hat{u}_p(\mu) \begin{bmatrix} 0 \\ W^T \hat{U}_p \\ 0 \end{bmatrix}, \end{aligned} \quad (3.16)$$

where Q_a, Q_u, Q_l are small positive integers, $Q_a^q(\mu), Q_l^k(\mu), \hat{u}_p(\mu): \Gamma \rightarrow \mathbb{R}$ are given functions that are easy to evaluate. In order to construct DDROM, we further simplify the ROM by defining $\tilde{M}_1 = V^T M_1 V$, $\tilde{M}_2 = W^T M_2 V$, $\tilde{M}_3 = W^T M_3 W$, $\tilde{K}^q = W^T K^q W$, $\tilde{\hat{U}}_p = W^T \hat{U}_p$, so that we have

$$\begin{aligned} & \left\{ \begin{bmatrix} 2\beta \tilde{M}_1 & 0 & -\tilde{M}_2^T \\ 0 & \tilde{M}_3 & 0 \\ -\tilde{M}_2 & 0 & 0 \end{bmatrix} + \sum_{q=1}^{Q_a} Q_a^q(\mu) \begin{bmatrix} 0 & 0 & 0 \\ 0 & 0 & (\tilde{K}^q)^T \\ 0 & \tilde{K}^q & 0 \end{bmatrix} \right\} \hat{x}(\mu) \\ &= \begin{bmatrix} 0 \\ 0 \\ \tilde{d} \end{bmatrix} + \sum_{p=1}^{Q_u} \hat{u}_p(\mu) \begin{bmatrix} 0 \\ \tilde{\hat{U}}_p \\ 0 \end{bmatrix}, \end{aligned} \quad (3.17)$$

and

$$\widehat{y}(\mu) = \sum_{k=1}^{Q_l} Q_l^k(\mu) C_k \begin{bmatrix} V^T & 0 & 0 \\ 0 & W^T & 0 \\ 0 & 0 & W^T \end{bmatrix} \widehat{x}(\mu) := \sum_{k=1}^{Q_l} Q_l^k(\mu) \widetilde{C}_k \widehat{x}(\mu). \quad (3.18)$$

Inspired by this formulation, in the \mathcal{L}_2 -optimal DDROM setting, we search for a structured DDROM with parameter-separable form as follows,

$$\begin{aligned} & \left\{ \begin{bmatrix} 2\beta \widetilde{M}_1 & 0 & -\widetilde{M}_2^T \\ 0 & \widetilde{M}_3 & 0 \\ -\widetilde{M}_2 & 0 & 0 \end{bmatrix} + \sum_{q=1}^{Q_{\tilde{a}}} \widetilde{Q}_a^q(\mu) \begin{bmatrix} 0 & 0 & 0 \\ 0 & 0 & (\widetilde{K}^q)^T \\ 0 & \widetilde{K}^q & 0 \end{bmatrix} \right\} \widehat{x}(\mu) \\ &= \begin{bmatrix} 0 \\ 0 \\ \tilde{d} \end{bmatrix} + \sum_{p=1}^{Q_{\tilde{u}}} \widetilde{u}_p(\mu) \begin{bmatrix} 0 \\ \widetilde{U}_p \\ 0 \end{bmatrix}, \end{aligned} \quad (3.19)$$

and

$$\widehat{y}(\mu) = \sum_{k=1}^{Q_{\tilde{l}}} \widetilde{Q}_l^k(\mu) \widetilde{C}_k \widehat{x}(\mu), \quad (3.20)$$

where $Q_{\tilde{a}}, Q_{\tilde{u}}, Q_{\tilde{l}}$ are small positive integers, $\widetilde{Q}_a^q(\mu), \widetilde{Q}_l^k(\mu), \widetilde{u}_p(\mu): \Gamma \rightarrow \mathbb{R}$ are given functions, and $\widetilde{M}_i (i = 1, 2, 3)$, $\widetilde{K}^q (q = 1, \dots, Q_{\tilde{a}})$, $\tilde{d}, \widetilde{U}_p (p = 1, \dots, Q_{\tilde{u}})$ and $\widetilde{C}_k (k = 1, \dots, Q_{\tilde{l}})$ are DDROM matrices what we want to get by minimizing the \mathcal{L}_2 error (3.12).

Note that the subtle difference between (3.17) and (3.19) is the "tilded" scalar functions, which aims to highlight that unlike in the projection-based ROM, where the scalar functions match those of the FOM, but in the DDROM, we have freedom in choosing them.

Reviewing the initial idea of this method, it is interested in approximating a input-to-output mapping (3.4) by a DDROM (3.10). The most important thing is that the framework does not need the full-order matrices and the full-order state x , but we only need the output y .

For the following explanation, a assumption is given first, and this assumption is easy to establish in most problems.

Assumption 3.1. *Let $(\Gamma, \Sigma, \mathbb{P})$ be a measure space, the functions $\widetilde{Q}_a^q(\mu), \widetilde{Q}_l^k(\mu), \widetilde{u}_p(\mu)$ are measurable, and satisfy*

$$\int_{\Gamma} \left\{ \frac{(1 + \sum_{p=1}^{Q_{\tilde{u}}} |\widetilde{u}_p(\mu)|) \sum_{k=1}^{Q_{\tilde{l}}} |\widetilde{Q}_l^k(\mu)|}{1 + \sum_{q=1}^{Q_{\tilde{a}}} |\widetilde{Q}_a^q(\mu)|} \right\}^2 d\mathbb{P}(\mu) < \infty. \quad (3.21)$$

Nextly, we introduce the set of allowable DDROM matrices based on Assumption 3.1, before that, we introduce some new notations for the structured DDROM (3.19), defining

$$\widetilde{A}_0 := \begin{bmatrix} 2\beta \widetilde{M}_1 & 0 & -\widetilde{M}_2^T \\ 0 & \widetilde{M}_3 & 0 \\ -\widetilde{M}_2 & 0 & 0 \end{bmatrix}, \widetilde{A}_q := \begin{bmatrix} 0 & 0 & 0 \\ 0 & 0 & (\widetilde{K}^q)^T \\ 0 & \widetilde{K}^q & 0 \end{bmatrix}, \widetilde{B}_0 := \begin{bmatrix} 0, 0, \tilde{d} \end{bmatrix}^T, \widetilde{B}_p := \begin{bmatrix} 0, \widetilde{U}_p, 0 \end{bmatrix}^T,$$

for $q = 1, \dots, Q_{\tilde{a}}$ and $p = 1, \dots, Q_{\tilde{u}}$.

Definition 3.2. Let R be the set of all tuples of DDROM matrices

$$(\tilde{A}_0, \tilde{A}_1, \dots, \tilde{A}_{Q_{\tilde{a}}}, \tilde{B}_0, \tilde{B}_1, \dots, \tilde{B}_{Q_{\tilde{u}}}, \tilde{C}_1, \dots, \tilde{C}_{Q_{\tilde{l}}}) =: (\tilde{A}_p, \tilde{B}_q, \tilde{C}_k),$$

for $p = 0, 1, \dots, Q_{\tilde{a}}$, $q = 0, 1, \dots, Q_{\tilde{u}}$ and $k = 1, 2, \dots, Q_{\tilde{l}}$. Then we define the set \mathcal{R} of allowable DDROM matrices as

$$\mathcal{R} = \left\{ (\tilde{A}_p, \tilde{B}_q, \tilde{C}_k) \in R : \text{ess sup}_{\mu \in \Gamma} \left\| (1 + \tilde{Q}_a^q(\mu))(\tilde{A}_0 + \sum_{q=1}^{Q_{\tilde{a}}} \tilde{Q}_a^q(\mu) \tilde{A}_q)^{-1} \right\|_{\mathcal{F}} < \infty \right\}. \quad (3.22)$$

It is important to establish that the set \mathcal{R} is open and that it forms a set of feasible DDROMs for the following analysis, the lemma gives the corresponding conclusions.

Lemma 3.3. The set \mathcal{R} (3.22) in Definition 3.2 is open. Moreover, for all \hat{y} defined by a DDROM $(\tilde{A}_p, \tilde{B}_q, \tilde{C}_k) \in \mathcal{R}$, we have that \hat{y} is square-integrable.

3.3 The gradients of the \mathcal{L}_2 approximation error

Based on the previous conclusions, in this section, we will derive the gradients of the \mathcal{L}_2 cost function (3.12) with respect to DDROM matrices $\tilde{A}_p, \tilde{B}_q, \tilde{C}_k$, these gradient formulas form the basis of our developed \mathcal{L}_2 -optimal reduced-order modeling algorithm which will be elaborated in next subsection.

We need to find the DDROM belonging to \mathcal{R} from Definition 3.2, because the Lemma 3.3 ensures that the square \mathcal{L}_2 error is clearly defined and differentiable on \mathcal{R} . Therefore, We don't continue to find the gradients for \mathcal{L}_2 (3.12), but for the following \mathcal{L}_2 -optimization problem

$$\underset{(\tilde{A}_p, \tilde{B}_q, \tilde{C}_k) \in \mathcal{R}}{\text{minimize}} \quad \mathcal{J}(\tilde{A}_p, \tilde{B}_q, \tilde{C}_k) = \|y - \hat{y}\|_{\mathcal{L}_2(\Gamma, \mathbb{P})}^2. \quad (3.23)$$

Now recall some contents will be used before giving the related theorem about the gradient's explicit expression. Firstly, we employ the reduced-order dual state $\hat{x}_d(\mu)$, which satisfies the reduced-order dual state equation

$$\begin{aligned} & \left\{ \begin{bmatrix} 2\beta \tilde{M}_1^T & 0 & -\tilde{M}_2^T \\ 0 & \tilde{M}_3^T & 0 \\ -\tilde{M}_2 & 0 & 0 \end{bmatrix} + \sum_{q=1}^{Q_{\tilde{a}}} \tilde{Q}_a^q(\mu) \begin{bmatrix} 0 & 0 & 0 \\ 0 & 0 & \tilde{K}^q \\ 0 & (\tilde{K}^q)^T & 0 \end{bmatrix} \right\} \hat{x}_d(\mu) \\ &= \sum_{k=1}^{Q_{\tilde{l}}} \tilde{Q}_l^k(\mu) (\tilde{C}^k)^T. \end{aligned} \quad (3.24)$$

Next, for a Fréchet differentiable function $f : U \rightarrow \mathbb{R}$, defined on an open subset U of a Hilbert space H with inner product $\langle \cdot, \cdot \rangle$, the gradient of f at x , denoted $\nabla f(x)$, is the unique element of H satisfying $f(x + h) = f(x) + \langle \nabla f(x), h \rangle + o(\|h\|)$, where $g(h) = o(\|h\|)$ denotes that $\lim_{h \rightarrow 0} \frac{g(h)}{\|h\|} = 0$. For a multivariate function $f(x_1, x_2, \dots, x_k)$, partial gradients $\nabla_{x_i} f(x_1, x_2, \dots, x_k)$ are defined in a similar way.

Theorem 3.4. Let $(\tilde{A}_p, \tilde{B}_q, \tilde{C}_k)$ be a tuple of DDROM matrices belonging to \mathcal{R} which is defined in Definition 3.2. Then the gradients of \mathcal{J} with respect to the DDROM matrices are

$$\begin{aligned}\nabla_{\tilde{A}_0} \mathcal{J} &= 2 \int_{\Gamma} \hat{x}_d(\mu) [y(\mu) - \hat{y}(\mu)] \hat{x}^T(\mu) d\mathbb{P}(\mu), \\ \nabla_{\tilde{A}_q} \mathcal{J} &= 2 \int_{\Gamma} \tilde{Q}_a^q(\mu) \hat{x}_d(\mu) [y(\mu) - \hat{y}(\mu)] \hat{x}^T(\mu) d\mathbb{P}(\mu), \quad q = 1, 2, \dots, Q_{\tilde{a}}, \\ \nabla_{\tilde{B}_0} \mathcal{J} &= 2 \int_{\Gamma} \hat{x}_d(\mu) [\hat{y}(\mu) - y(\mu)] d\mathbb{P}(\mu), \\ \nabla_{\tilde{B}_p} \mathcal{J} &= 2 \int_{\Gamma} \tilde{Q}_u^p(\mu) \hat{x}_d(\mu) [\hat{y}(\mu) - y(\mu)] d\mathbb{P}(\mu), \quad p = 1, 2, \dots, Q_{\tilde{u}}, \\ \nabla_{\tilde{C}_k} \mathcal{J} &= 2 \int_{\Gamma} \tilde{Q}_l^k(\mu) [\hat{y}(\mu) - y(\mu)] \hat{x}^T(\mu) d\mathbb{P}(\mu), \quad k = 1, 2, \dots, Q_{\tilde{l}}.\end{aligned}$$

Proof. Firstly, in order to simplify the symbolic representation in the process of proof, we will write (3.19) and (3.20) as

$$\begin{aligned}\mathbf{A}(\mu) \hat{x}(\mu) &= \mathbf{B}(\mu), \\ \hat{y}(\mu) &= \mathbf{C}(\mu) \hat{x}(\mu).\end{aligned}\tag{3.25}$$

where

$$\begin{aligned}\mathbf{A}(\mu) &= \tilde{A}_0 + \sum_{q=1}^{Q_{\tilde{a}}} \tilde{Q}_a^q(\mu) \tilde{A}_q := \sum_{q=0}^{Q_{\tilde{a}}} \tilde{Q}_a^q(\mu) \tilde{A}_q, \\ \mathbf{B}(\mu) &= \tilde{B}_0 + \sum_{p=1}^{Q_{\tilde{u}}} \tilde{Q}_u^p(\mu) \tilde{B}_p := \sum_{p=0}^{Q_{\tilde{u}}} \tilde{Q}_u^p(\mu) \tilde{B}_p, \\ \mathbf{C}(\mu) &= \sum_{k=1}^{Q_{\tilde{l}}} \tilde{Q}_l^k(\mu) \tilde{C}_k,\end{aligned}$$

and $\tilde{Q}_a^0 = \tilde{Q}_u^0 = 1$. After that bringing $\hat{y}(\mu) = \mathbf{C}(\mu) \mathbf{A}^{-1}(\mu) \mathbf{B}(\mu)$ from (3.25) into the objective function, with $\langle y, \hat{y} \rangle_{\mathcal{L}_2(\Gamma, \mathbb{P})} = \langle \hat{y}, y \rangle_{\mathcal{L}_2(\Gamma, \mathbb{P})}$ we have

$$\begin{aligned}\mathcal{J} &= \|y - \hat{y}\|_{\mathcal{L}_2(\Gamma, \mathbb{P})}^2 \\ &= \|y\|_{\mathcal{L}_2(\Gamma, \mathbb{P})}^2 - 2\langle y, \hat{y} \rangle_{\mathcal{L}_2(\Gamma, \mathbb{P})} + \|\hat{y}\|_{\mathcal{L}_2(\Gamma, \mathbb{P})}^2 \\ &= \|y\|_{\mathcal{L}_2(\Gamma, \mathbb{P})}^2 - 2 \int_{\Gamma} \text{tr} (y^T(\mu) \mathbf{C}(\mu) \mathbf{A}^{-1}(\mu) \mathbf{B}(\mu)) d\mathbb{P}(\mu) \\ &\quad + \int_{\Gamma} \text{tr} (\mathbf{B}^T(\mu) \mathbf{A}^{-T}(\mu) \mathbf{C}^T(\mu) \mathbf{C}(\mu) \mathbf{A}^{-1}(\mu) \mathbf{B}(\mu)) d\mathbb{P}(\mu).\end{aligned}\tag{3.26}$$

The first part of the (3.26) has nothing to do with the solution of gradient, so it will not be considered in the future. Record the remaining two items as \mathcal{J}_2 and \mathcal{J}_3 respectively, i.e.

$$\begin{aligned}\mathcal{J}_2 &= -2 \int_{\Gamma} \text{tr} (y^T(\mu) \mathbf{C}(\mu) \mathbf{A}^{-1}(\mu) \mathbf{B}(\mu)) d\mathbb{P}(\mu), \\ \mathcal{J}_3 &= \int_{\Gamma} \text{tr} (\mathbf{B}^T(\mu) \mathbf{A}^{-T}(\mu) \mathbf{C}^T(\mu) \mathbf{C}(\mu) \mathbf{A}^{-1}(\mu) \mathbf{B}(\mu)) d\mathbb{P}(\mu).\end{aligned}$$

Next, find the gradients of the above two terms about \tilde{A}_q , \tilde{B}_p and \tilde{C}_k respectively. Taking $\nabla_{\tilde{A}_q} \mathcal{J}_2$ as an example, we will describe it in detail. To do so, we evaluate $\mathcal{J}_2(\tilde{A}_q + \Delta \tilde{A}_q)$ for a perturbation $\Delta \tilde{A}_q$ which is small enough. Besides that, we need using the property in (3.22), and applying the Neumann series formula yield.

$$\begin{aligned}
\mathcal{J}_2(\tilde{A}_q + \Delta \tilde{A}_q) &= -2 \int_{\Gamma} \text{tr} \left(y^T(\mu) \mathbf{C}(\mu) (\mathbf{A}(\mu) + \tilde{Q}_a^q(\mu) \Delta \tilde{A}_q)^{-1} \mathbf{B}(\mu) \right) d\mathbb{P}(\mu) \\
&= -2 \int_{\Gamma} \text{tr} \left(y^T(\mu) \mathbf{C}(\mu) \left(I + \tilde{Q}_a^q(\mu) \mathbf{A}^{-1}(\mu) \Delta \tilde{A}_q \right)^{-1} \mathbf{A}^{-1}(\mu) \mathbf{B}(\mu) \right) d\mathbb{P}(\mu) \\
&= -2 \int_{\Gamma} \text{tr} \left(y^T(\mu) \mathbf{C}(\mu) \mathbf{A}^{-1}(\mu) \mathbf{B}(\mu) \right) d\mathbb{P}(\mu) \\
&\quad + 2 \int_{\Gamma} \text{tr} \left(\tilde{Q}_a^q(\mu) y^T(\mu) \mathbf{C}(\mu) \mathbf{A}^{-1}(\mu) \Delta \tilde{A}_q \mathbf{A}^{-1}(\mu) \mathbf{B}(\mu) \right) d\mathbb{P}(\mu) \\
&\quad - 2 \int_{\Gamma} \text{tr} \left(y^T(\mu) \mathbf{C}(\mu) \sum_{m=2}^{\infty} \left(-\tilde{Q}_a^q(\mu) \mathbf{A}^{-1}(\mu) \Delta \tilde{A}_q \right)^m \mathbf{A}^{-1}(\mu) \mathbf{B}(\mu) \right) d\mathbb{P}(\mu) \\
&= \mathcal{J}_2(\tilde{A}_q) + \left\langle 2 \int_{\Gamma} \tilde{Q}_a^q(\mu) \mathbf{A}^{-T}(\mu) \mathbf{C}^T(\mu) y(\mu) \mathbf{B}^T(\mu) \mathbf{A}^{-T}(\mu) d\mathbb{P}(\mu), \Delta \tilde{A}_q \right\rangle_{\mathcal{F}} \\
&\quad - 2 \sum_{m=2}^{\infty} \int_{\Gamma} \text{tr} \left(y^T(\mu) \mathbf{C}(\mu) \left(-\tilde{Q}_a^q(\mu) \mathbf{A}^{-1}(\mu) \Delta \tilde{A}_q \right)^m \mathbf{A}^{-1}(\mu) \mathbf{B}(\mu) \right) d\mathbb{P}(\mu).
\end{aligned}$$

Observing the last equation, to get $\nabla_{\tilde{A}_q} \mathcal{J}_2$, we need to prove that the second term is bounded, and the third term is about the low-order infinitesimal of $\Delta \tilde{A}_q$. In the process of proving that the second term is bounded, we will use (3.22),

$$\begin{aligned}
&\left\| \int_{\Gamma} \tilde{Q}_a^q(\mu) \mathbf{A}^{-T}(\mu) \mathbf{C}^T(\mu) y(\mu) \mathbf{B}^T(\mu) \mathbf{A}^{-T}(\mu) d\mathbb{P}(\mu) \right\|_{\mathcal{F}} \\
&\leq \int_{\Gamma} |\tilde{Q}_a^q(\mu)| \|\mathbf{A}^{-1}(\mu)\|_{\mathcal{F}} \|\mathbf{C}(\mu)\|_{\mathcal{F}} \|\mathbf{A}^{-1}(\mu)\|_{\mathcal{F}} \|\mathbf{B}(\mu)\|_{\mathcal{F}} \|y(\mu)\|_{\mathcal{F}} d\mathbb{P}(\mu) \\
&\leq \|\tilde{Q}_a^q(\mu)(\tilde{A}_0 + \sum_{q=1}^{Q_{\tilde{a}}} \tilde{Q}_a^q(\mu) \tilde{A}_q)^{-1}\|_{\mathcal{L}_{\infty}(\Gamma, \mathbb{P})} \int_{\Gamma} \|\mathbf{C}(\mu)\|_{\mathcal{F}} \|\mathbf{A}^{-1}(\mu)\|_{\mathcal{F}} \|\mathbf{B}(\mu)\|_{\mathcal{F}} \|y(\mu)\|_{\mathcal{F}} d\mathbb{P}(\mu) \\
&< \infty.
\end{aligned}$$

Then we prove that the last term is of low order,

$$\begin{aligned}
& \left| \sum_{m=2}^{\infty} \int_{\Gamma} \text{tr} \left(y^T(\mu) \mathbf{C}(\mu) \left(-\tilde{Q}_a^q(\mu) \mathbf{A}^{-1}(\mu) \Delta \tilde{A}_q \right)^m \mathbf{A}^{-1}(\mu) \mathbf{B}(\mu) \right) d\mathbb{P}(\mu) \right| \\
& \leq \|y(\mu)\|_{\mathcal{L}_2(\Gamma, \mathbb{P})} \sum_{m=2}^{\infty} \left\| \mathbf{C}(\mu) \left(-\tilde{Q}_a^q(\mu) \mathbf{A}^{-1}(\mu) \Delta \tilde{A}_q \right)^m \mathbf{A}^{-1}(\mu) \mathbf{B}(\mu) \right\|_{\mathcal{L}_2(\Gamma, \mathbb{P})} \\
& \leq \|y(\mu)\|_{\mathcal{L}_2(\Gamma, \mathbb{P})} \sum_{m=2}^{\infty} \left\| \tilde{Q}_a^q(\mu) \mathbf{A}^{-1}(\mu) \right\|_{\mathcal{L}_{\infty}}^m \left\| \|\mathbf{C}(\mu)\|_{\mathcal{F}} \|\mathbf{A}^{-1}(\mu)\|_{\mathcal{F}} \|\mathbf{B}(\mu)\|_{\mathcal{F}} \right\|_{\mathcal{L}_2(\Gamma, \mathbb{P})} \|\Delta \tilde{A}_q\|_{\mathcal{F}}^m \\
& = \|y(\mu)\|_{\mathcal{L}_2(\Gamma, \mathbb{P})} \left\| \|\mathbf{C}(\mu)\|_{\mathcal{F}} \|\mathbf{A}^{-1}(\mu)\|_{\mathcal{F}} \|\mathbf{B}(\mu)\|_{\mathcal{F}} \right\|_{\mathcal{L}_2(\Gamma, \mathbb{P})} \frac{\left\| \tilde{Q}_a^q(\mu) \mathbf{A}^{-1}(\mu) \right\|_{\mathcal{L}_{\infty}}^2 \|\Delta \tilde{A}_q\|_{\mathcal{F}}^2}{1 - \left\| \tilde{Q}_a^q(\mu) \mathbf{A}^{-1}(\mu) \right\|_{\mathcal{L}_{\infty}} \|\Delta \tilde{A}_q\|_{\mathcal{F}}} \\
& = o \left(\|\Delta \tilde{A}_q\|_{\mathcal{F}} \right).
\end{aligned}$$

According to the above proof, we get the expression of $\nabla_{\tilde{A}_q} \mathcal{J}_2$, i.e.

$$\nabla_{\tilde{A}_q} \mathcal{J}_2 = 2 \int_{\Gamma} \tilde{Q}_a^q(\mu) \mathbf{A}^{-T}(\mu) \mathbf{C}^T(\mu) y(\mu) \mathbf{B}^T(\mu) \mathbf{A}^{-T}(\mu) d\mathbb{P}(\mu),$$

especially,

$$\nabla_{\tilde{A}_0} \mathcal{J}_2 = 2 \int_{\Gamma} \mathbf{A}^{-T}(\mu) \mathbf{C}^T(\mu) y(\mu) \mathbf{B}^T(\mu) \mathbf{A}^{-T}(\mu) d\mathbb{P}(\mu).$$

If we want to get the expression of $\nabla_{\tilde{B}_p} \mathcal{J}_2$, we need evaluating $\mathcal{J}_2 \left(\tilde{B}_p + \Delta \tilde{B}_p \right)$,

$$\begin{aligned}
\mathcal{J}_2 \left(\tilde{B}_p + \Delta \tilde{B}_p \right) & = -2 \int_{\Gamma} \text{tr} \left(y^T(\mu) \mathbf{C}(\mu) \mathbf{A}^{-1}(\mu) \left(\mathbf{B}(\mu) + \tilde{Q}_u^p(\mu) \Delta \tilde{B}_p \right) \right) d\mathbb{P}(\mu) \\
& = \mathcal{J}_2(\tilde{B}_p) - 2 \int_{\Gamma} \text{tr} \left(\tilde{Q}_u^p(\mu) y^T(\mu) \mathbf{C}(\mu) \mathbf{A}^{-1}(\mu) \Delta \tilde{B}_p \right) d\mathbb{P}(\mu) \\
& = \mathcal{J}_2(\tilde{B}_p) - 2 \left\langle \int_{\Gamma} \tilde{Q}_u^p(\mu) \mathbf{A}^{-T}(\mu) \mathbf{C}^T(\mu) y(\mu) d\mathbb{P}(\mu) \Delta \tilde{B}_p \right\rangle_{\mathcal{F}},
\end{aligned}$$

therefore

$$\nabla_{\tilde{B}_p} \mathcal{J}_2 = -2 \int_{\Gamma} \tilde{Q}_u^p(\mu) \mathbf{A}^{-T}(\mu) \mathbf{C}^T(\mu) y(\mu) d\mathbb{P}(\mu),$$

especially,

$$\nabla_{\tilde{B}_0} \mathcal{J}_2 = -2 \int_{\Gamma} \mathbf{A}^{-T}(\mu) \mathbf{C}^T(\mu) y(\mu) d\mathbb{P}(\mu),$$

Similarly, we also can get

$$\nabla_{\tilde{C}_k} \mathcal{J}_2 = -2 \int_{\Gamma} \tilde{Q}_l^k(\mu) y(\mu) \mathbf{B}^T(\mu) \mathbf{A}^{-T}(\mu) d\mathbb{P}(\mu).$$

The above is the result of finding the gradient of the second term \mathcal{J}_2 . Similar to the steps of finding the gradients for \mathcal{J}_2 , and then finding the gradients for \mathcal{J}_3 , we won't

go into details here, and finally we can get the gradient for (3.26). The conclusion is as follows.

$$\begin{aligned}\nabla_{\tilde{A}_a^q} \mathcal{J} &= 2 \int_{\Gamma} \tilde{Q}_q(\mu) \mathbf{A}^{-T}(\mu) \mathbf{C}^T(\mu) (y(\mu) - \mathbf{C}(\mu) \mathbf{A}^{-1}(\mu) \mathbf{B}(\mu)) \mathbf{B}^T(\mu) \mathbf{A}^{-T}(\mu) d\mathbb{P}(\mu), \\ \nabla_{\tilde{B}_p} \mathcal{J} &= 2 \int_{\Gamma} \tilde{Q}_u^p(\mu) \mathbf{A}^{-T}(\mu) \mathbf{C}^T(\mu) (\mathbf{C}(\mu) \mathbf{A}^{-1}(\mu) \mathbf{B}(\mu) - y(\mu)) d\mathbb{P}(\mu), \\ \nabla_{\tilde{C}_k} \mathcal{J} &= 2 \int_{\Gamma} \tilde{Q}_l^k(\mu) (\mathbf{C}(\mu) \mathbf{A}^{-1}(\mu) \mathbf{B}(\mu) - y(\mu)) \mathbf{B}^T(\mu) \mathbf{A}^{-T}(\mu) d\mathbb{P}(\mu).\end{aligned}$$

Bring in $\hat{y}(\mu) = \mathbf{C}(\mu) \mathbf{A}^{-1}(\mu) \mathbf{B}(\mu)$ and $\hat{x}_d(\mu) = \mathbf{A}^{-1}(\mu) \mathbf{C}(\mu)$, we get the conclusion in the Theorem 3.4. \square

Obviously, the gradients obtained by the Theorem 3.4 do not need to access the full-order matrices M_i , K^q , \hat{U}_p and C_k or full-order state $x(\mu)$, but is directly calculated from the output $y(\mu)$ of the FOM. Through data-driven access to these gradient evaluations, we can design various optimization algorithms to build \mathcal{L}_2 -optimal DDROM for different situations, and the algorithm only needs to access the output $y(\mu)$ of the FOM. We will discuss the details of the algorithm in the next section.

Algorithm 1 \mathcal{L}_2 -Opt-PSF

Input: Input-to-output mapping y , initial guess for DDROM $(\tilde{A}_q, \tilde{B}_p, \tilde{C}_k)$, maximum number of iterations **maxit**, tolerance **tol** > 0 .

- 1: Set $\hat{y}^{(0)}$ as the output of the initial DDROM.
- 2: **for** i in $1, 2, \dots, \text{maxit}$ **do**
- 3: Compute a new DDROM with output $\hat{y}^{(i)}$ using a step of a gradient-based optimization method, with the squared \mathcal{L}_2 error in (3.12) as the objective function and gradients based on Theorem 3.4.
- 4: **if** $\frac{\|\hat{y}^{(i-1)} - \hat{y}^{(i)}\|_{\mathcal{L}_2(\Gamma, \mathbb{P})}}{\|\hat{y}^{(i)}\|_{\mathcal{L}_2(\Gamma, \mathbb{P})}} \leq \text{tol}$ **then**
- 5: Exit the **for** loop.
- 6: **end if**
- 7: **end for**
- 8: **return** the last computed DDROM.

Output: DDROM $(\tilde{A}_q, \tilde{B}_p, \tilde{C}_k)$.

3.4 The data-driven, gradient-based algorithm

In this section, we describe proposed \mathcal{L}_2 -optimal reduced-order modeling algorithm with separable parameters form (\mathcal{L}_2 -Opt-PSF). The pseudocode is given in Algorithm 1.

We give some details about the algorithm. For input, we use the initial matrices M_i , K^q , d , \hat{U}_p , and C_k to construct the initial guess for DDROM $(\tilde{A}_q, \tilde{B}_p, \tilde{C}_k)$. We don't specify the optimization method mentioned in the Algorithm 1, but for this non-convex optimization problem, we should choose an appropriate method and pay attention to the influence of the initial value on the final result. Because this method will not access the full order matrices and the full order state $x(\mu)$ in the FOM, we only use the relative change in output error when setting the stop criterion.

4 Generalized multiscale finite element method

In the section 3.4, we give the \mathcal{L}_2 -optimal reduced-order modeling algorithm. We need to provide an initial value for the algorithm to get the final DDROM. Given the full order matrix in the FOM, the ROM can be obtained by POD method or RB method. When these projection-based methods are used to construct ROMs, it is necessary to calculate (2.10) for many training samples to get the snapshot space.

Generally speaking, the number of training samples is very large, and it needs high calculation cost. Besides, the constraint in the optimization problem can be a partial differential equation with multiscale structure. As a local model reduction method, the generalized multiscale finite element method (GMsFEM) can effectively deal with these problems. One of the most important characteristics of GMsFEM is that multiscale basis functions can be calculated in offline stage and can be used repeatedly for models with different source terms, boundary conditions and similar multiscale structural coefficients. In this section, we will briefly outline the local model reduction using GMsFEM.

Before giving the detailed procedures of GMsFEM, we firstly set the scene of the numerical discretization. We assume that the computational domain Ω is partitioned uniformly by a coarse mesh \mathcal{T}_H and a fine mesh \mathcal{T}_h , with mesh size H and h , respectively. Moreover, \mathcal{T}_h is obtained by refining the coarse mesh \mathcal{T}_H . The nodes of the the coarse mesh are denoted by $\{N_i\}_{i=1}^{\mathcal{N}_c}$, $i = 1, \dots, \mathcal{N}_c$. The neighborhood ω_i of the node N_i consists of all the coarse mesh elements for which node N_i is a vertex, i.e.,

$$\omega_i = \cup \{K_s \in \mathcal{T}_H \mid x_i \in \bar{K}_s\},$$

each coarse grid is a unit K .

Generalized multiscale finite element method uses two stages: offline stage and online stage. At the offline stage of GMsFEM, we firstly construct the space of snapshots, $V_{snap}^{(i)}$, and then introduce the construction of local reduced basis functions. For the snapshot space, we can construct it by various ways: (1) all fine-grid functions; (2) harmonic snapshots; (3) oversampling harmonic snapshots; and (4) forced-based snapshots. In the following, we will introduce the first way to form the snapshot spaces.

Suppose \mathcal{L} is the differential operator corresponding to the state equation and adjoint equation in (2.5), and the state equation is a diffusion equation with diffusion coefficient $\kappa(x)$. Firstly, we solve the eigenvalue problem on each subdomain ω_i

$$\begin{cases} \mathcal{L}(\phi_{i,\ell}) = \lambda_{i,\ell} \widetilde{\kappa(x)} \phi_{i,\ell} & \text{in } \omega_i, \\ \kappa(x) \cdot \nabla \phi_{i,\ell} \cdot n = 0 & \text{on } \partial \omega_i. \end{cases} \quad (4.1)$$

This gives a set of snapshot functions $\{\phi_{i,\ell}\}$. Here $\widetilde{\kappa(x)} = \kappa(x) \sum_{i=1}^{\mathcal{N}_c} H^2 |\nabla \chi_i|^2$ and $\{\chi_i\}$ is a set of partition of unity functions.

Let $\{L_m\}$ denote the set of basis functions of the fine grid. After the FEM discretization, the snapshot equation (4.1) gives the following matrix eigenvalue problem

$$K \phi_{i,\ell} = \lambda S \phi_{i,\ell}, \quad (4.2)$$

where

$$(K)_{m,n} = (\kappa(x) \nabla L_m, \nabla L_n)_{L^2(\omega_i)}, \quad (S)_{m,n} = (\widetilde{\kappa(x)} L_m, L_n)_{L^2(\omega_i)}.$$

Then we choose the M_i lowermost eigenvalues and the corresponding eigenvectors of the eigenvalue problem (4.2), and denote the eigenvalues and eigenvectors by $\{\lambda_\ell^{\omega_i}\}$ and $\{\varphi_\ell^{\omega_i}\}$, respectively. The local snapshot space $V_{\text{snap}}(\omega_i) := \{\varphi_\ell^{\omega_i}, 1 \leq \ell \leq M_i\}$. Let $M = \sum_{i=1}^{N_c} M_i$ be the total number of eigenvectors for snapshots. We use the partition of unity functions to paste the snapshot functions and get the multiscale basis function space

$$V_H(\Omega) := \text{span}\{\varphi_k : 1 \leq k \leq M\} = \text{span}\{\varphi_{i,\ell} : \varphi_{i,\ell} = \chi_i \varphi_\ell^{\omega_i}, 1 \leq i \leq N_c, 1 \leq \ell \leq M_i\}.$$

The multiscale basis functions can be repeatedly used online. We can use a matrix R^G to store these basis functions, i.e.,

$$(R^G)^T = [\varphi_1, \varphi_2, \dots, \varphi_M], \quad (4.3)$$

where each φ_j denotes a column vector. We look at the GMsFEM closer in terms of matrix-vector multiplication. Let K_g and F_g be the stiffness matrix and the load vector on coarse grid, and u_H represents the coarse solution. The discrete formulation of state equation in (2.5) on coarse grid is as follows,

$$a(u_H, v; \mu) = (f, v; \mu), \quad \forall v \in V_H, \quad (4.4)$$

This leads to a matrix form

$$K_g \bar{u}_H = F_g, \quad (4.5)$$

where $K_g = R^G K (R^G)^T$, $F_g = R^G b$ (b represents the load-vector on fine grid). Then we downscale the coarse scale solution to fine scale solution by using multiscale basis functions,

$$u_H = (R^G)^T \bar{u}_H. \quad (4.6)$$

At the online stage, the multiscale basis functions can be repeatedly used, so that Compared with direct numerical simulation on fine grid, GMsFEM can significantly improve the computation efficiency. Then, we use the Algorithm 2 to give an overview of GMsFEM.

Algorithm 2 GMsFEM

Input: The model $a(u, v; \mu) = (f, v; \mu)$ defined in the domain Ω

Offline Stage:

- 1: Generate grid, i.e., fine mesh \mathcal{T}_h and coarse mesh \mathcal{T}_H ;
- 2: Construct snapshot space $V_{\text{snap}}(\omega_i)$ for computing offline space.;
- 3: Construct a low-dimensional offline space $V_H(\Omega)$ by performing dimension reduction in the space of global snapshots.

Online Stage:

- 4: Compute multiscale basis functions for each input parameter;
- 5: Solve the coarse-grid problem for any force term and boundary condition;
- 6: Use iterative solvers if necessary.

Next, we apply GMsFEM into the optimality system (2.10) i.e., finding $(u_H, f_H, \lambda_H) \in \mathcal{V}_0^H(\Omega) \times \mathcal{M}_h(\Omega) \times \mathcal{V}_0^H$ such that

$$\begin{cases} a(u_H, \tilde{u}_H; \mu) = (f_H, \tilde{u}_H; \mu), \forall \tilde{u}_H \in \mathcal{V}_0^H(\Omega), \\ a(\lambda_H, \tilde{\lambda}_H; \mu) = -(u_H - \hat{u}, \tilde{\lambda}_H; \mu), \forall \tilde{\lambda}_H \in \mathcal{V}_0^H(\Omega), \\ 2\beta(f_H, \tilde{f}_H; \mu) = (\tilde{f}_H, \lambda_H; \mu), \forall \tilde{f}_H \in \mathcal{M}_h(\Omega), \end{cases} \quad (4.7)$$

where $\mathcal{V}_0^H(\Omega) := V_H(\Omega) \otimes L^2(\Gamma) \subset \mathcal{V}_0^h(\Omega)$. The reduced optimality matrix corresponding to (4.7) is

$$\underbrace{\begin{bmatrix} 2\beta M_1 & 0 & -M_2^T R^G \\ 0 & (R^G)^T M_3 R^G & (R^G)^T K^T(\mu) R^G \\ -(R^G)^T M_2 & (R^G)^T K(\mu) R^G & 0 \end{bmatrix}}_{\mathcal{A}_H(\mu) \in \mathbb{R}^{(2M+N_e) \times (2M+N_e)}} \begin{bmatrix} \bar{F}_H(\mu) \\ \bar{U}_H(\mu) \\ \bar{\Lambda}_H(\mu) \end{bmatrix} = \begin{bmatrix} 0 \\ (R^G)^T \bar{U}(\mu) \\ (R^G)^T d \end{bmatrix}, \quad (4.8)$$

If we set

$$R = \begin{bmatrix} I & 0 & 0 \\ 0 & (R^G)^T & 0 \\ 0 & 0 & (R^G)^T \end{bmatrix} \in \mathbb{R}^{(2M+N_e) \times (2M+N_e)},$$

we can get $\mathcal{A}_H(\mu) = R \mathcal{A}_h(\mu) R^T$, and then

$$\begin{aligned} F_H(\mu) &= (R^G)^T \bar{F}_H(\mu), \\ U_H(\mu) &= (R^G)^T \bar{U}_H(\mu), \\ \Lambda_H(\mu) &= (R^G)^T \bar{\Lambda}_H(\mu). \end{aligned}$$

(4.8) can be transformed into the form of variable separation, so it can be converted into the forms similar to (3.14) and (3.15) by introducing the interest quantity, so we get the FOM using GMsFEM.

5 Numerical examples

In this section, we present results of two numerical experiments to illustrate the effectiveness of \mathcal{L}_2 -Opt-PSF(Algorithm 1) in solving stochastic optimal control problems, in which PDE constraints, objective functional and control constraints under different parameter settings are studied. In particular, we focus on the case of a one-dimensional parameter.

Given a training set $\mathcal{P}_{train} \subset \mathcal{P} = [1, 10]$ and a FOM, ROM is constructed by Galerkin projection method as the initial value of the algorithm. In the numerical experiment, we generated a training set by uniformly sampling 100 data points from the interval $[1, 10]$ for the parameter values. Specifically, we used linearly spaced sampling to ensure a comprehensive coverage of the parameter space and to provide sufficient diversity for model training. This process was implemented using MATLAB's linspace function, which generates an array of evenly spaced values over a specified interval.

The Broyden–Fletcher–Goldfarb–Shanno (BFGS) algorithm with a strong Wolfe line search strategy is chosen for the gradient-based optimization method in Algorithm

[1](#) to speed up the convergence, where the maximum number of iterations (**maxit**) and tolerance (**tol**) for BFGS are set to 1000 and 10^{-16} respectively.

When the mesh generation process is encrypted and the training data set is large, using the FEM to calculate the snapshot space can significantly reduce computational efficiency. To address this issue, we adopt the GMsFEM discussed in Chapter [4](#) to enhance computational performance. It leverages GMsFEM's ability to capture fine grid features on a coarser grid, thereby reducing computational complexity while maintaining accuracy.

5.1 Optimal control for stochastic diffusion equation

We start with the following stochastic optimal control problem defined on the two-dimensional unit square $\Omega = [0, 1]^2$:

$$\begin{cases} \min_{u,f} J(u, f) = \frac{1}{2} \|u(x, \mu) - \hat{u}(x, \mu)\|_{\mathcal{L}^2(\Omega)}^2 + \beta \|f(x, \mu)\|_{\mathcal{L}^2(\Omega)}^2, \\ \text{s.t. } -\operatorname{div}(\kappa(x, \mu) \nabla u(x, \mu)) = f(x, \mu), \text{ in } \Omega, \\ \quad u(x, \mu) = 0, \text{ on } \partial\Omega, \end{cases} \quad (5.1)$$

where $\beta = 10^{-3}$, the diffusion coefficient $\kappa(x, \mu)$ and the desired state function $\hat{u}(x, \mu)$ are

$$\begin{cases} \kappa(x, \mu) = \kappa_1(x) + \mu(1 - x_1) \\ \hat{u}(x, \mu) = x_1 x_2 (1 - x_1) (1 - x_2) + \mu x_1^2 x_2^2 (1 - x_1) (1 - x_2) \end{cases}$$

Here $x = (x_1, x_2) \in \Omega$, $\kappa_1(x)$ is a high-contrast function and its map is depicted in Figure [1](#)

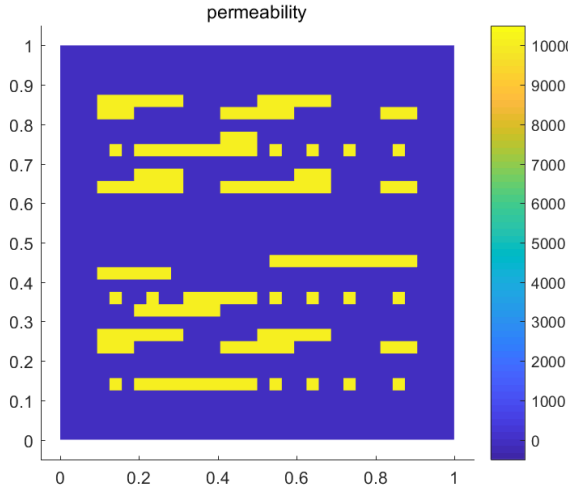


Figure 1: High-contrast coefficient κ_1

First, for the FOM, we use the FEM on a 64×64 uniform fine grid to compute the reference solutions $(F_{ref}, U_{ref}, \Lambda_{ref})$ and obtain the snapshot space. We then select a snapshot matrix to derive the ROM with $r = 3$, which serves as the initial value for the

algorithm. For the output in the model, we let

$$y(\mu) = \left\{ \begin{bmatrix} 0 \\ 0 \\ d \end{bmatrix} + \mu \begin{bmatrix} 0 \\ \widehat{U}_p \\ 0 \end{bmatrix} \right\} x(\mu).$$

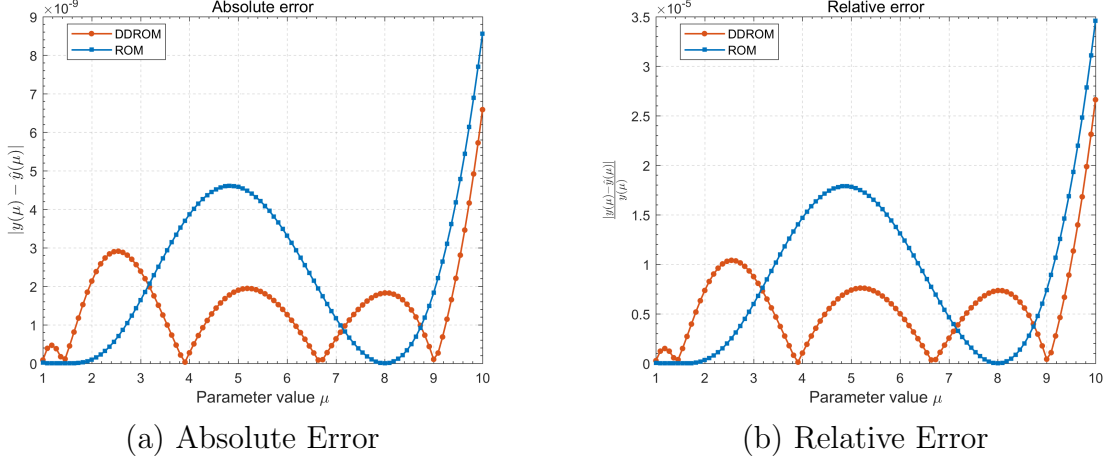


Figure 2: Error plots for the quantity of interest y with the finite element solution $y(\mu)$ as the reference, where $\hat{y}(\mu)$ is the interest of the reduced-order model.

Since the optimal control problem pays more attention to U and F in (2.13), we need to adjust the matrix C in (3.3) so that the output $y(\mu)$ is only related to U or F . Obviously, we only need to let $y(\mu)$ have the following form respectively,

$$y(\mu) = \left\{ \begin{bmatrix} 0 \\ I \\ 0 \end{bmatrix} + \mu \begin{bmatrix} 0 \\ 0 \\ 0 \end{bmatrix} \right\} x(\mu),$$

$$y(\mu) = \left\{ \begin{bmatrix} I \\ 0 \\ 0 \end{bmatrix} + \mu \begin{bmatrix} 0 \\ 0 \\ 0 \end{bmatrix} \right\} x(\mu).$$

The relative error plots are shown in the following figure.

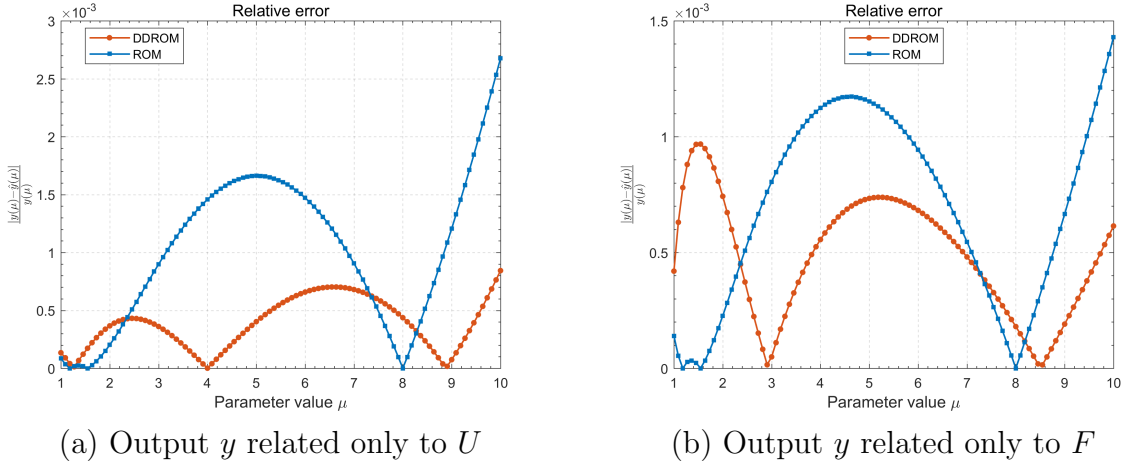


Figure 3: Relative error plots for the quantity of interest y related only to U or F .

Then, we use a 128×128 uniform fine grid to calculate the reference solutions. For the data-driven model reduction, the solutions are computed on an 8×8 coarse mesh.

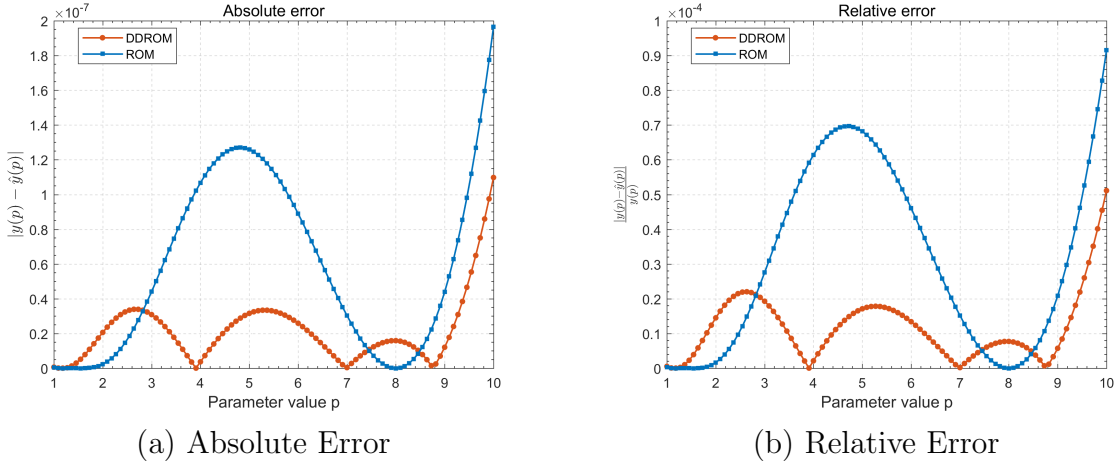


Figure 4: Error plots for the quantity of interest y .

The above error images reflect the effectiveness of the method to obtain DDROM, and then we give the images with the solutions at $\bar{\mu}$.

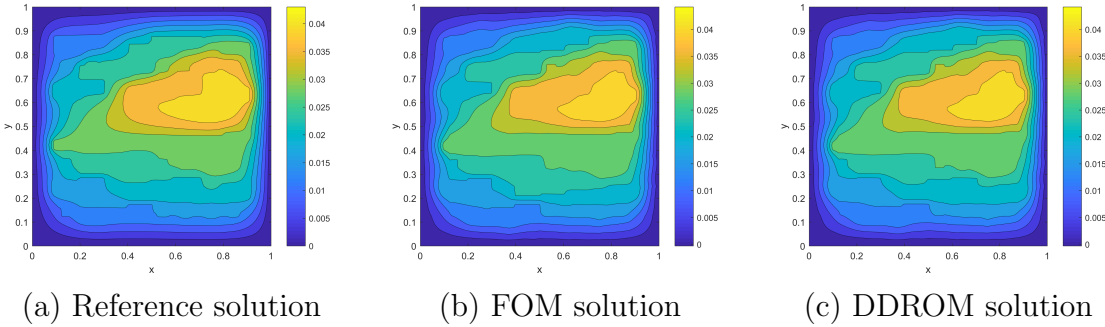


Figure 5: Images of solution U at $\bar{\mu}$.

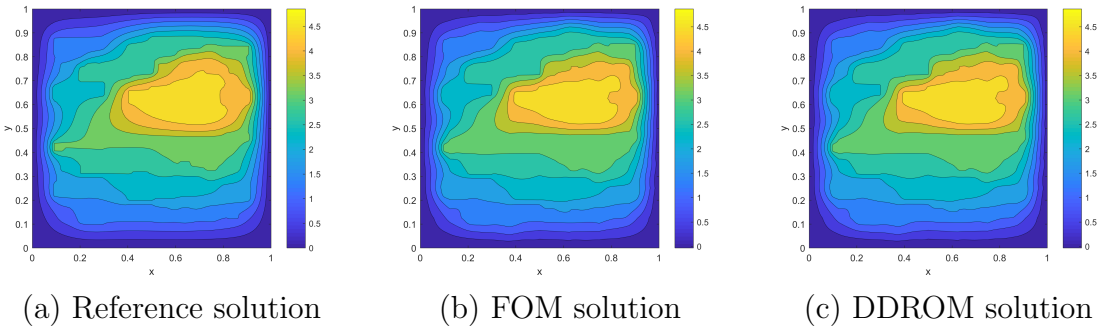


Figure 6: Images of solution F at $\bar{\mu}$.

The uniform fine mesh of 128×128 is fixed and the coarse mesh is refined to 16×16 , and then we give the images with the solutions of U and F at $\bar{\mu}$.

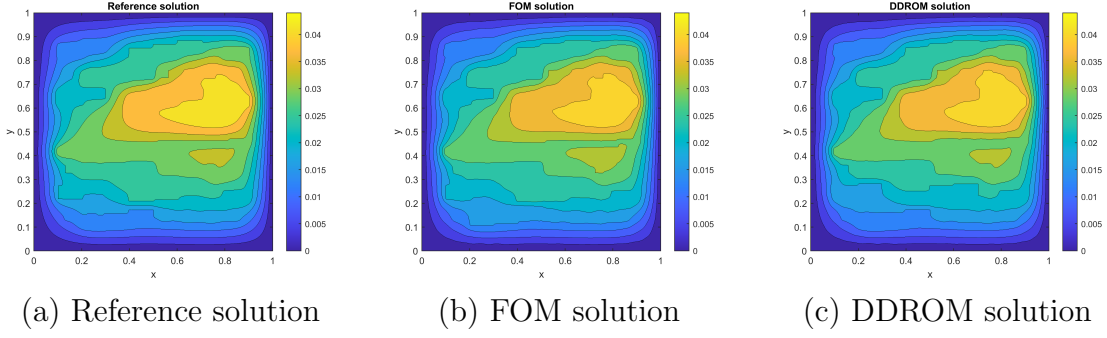


Figure 7: Images of solution U at $\bar{\mu}$.

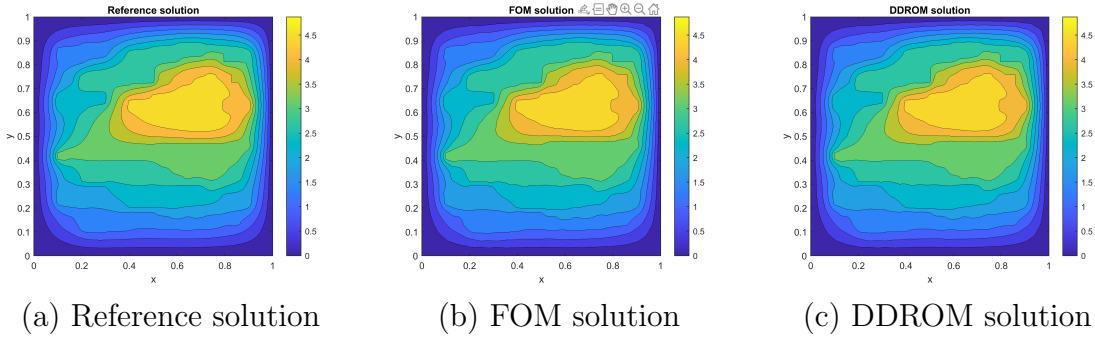


Figure 8: Images of solution F at $\bar{\mu}$.

5.2 Optimal control for stochastic advection-diffusion equation

In this case, we take the stochastic advection-diffusion equation as a constraint. We start with the following stochastic optimal control problem defined on the two-dimensional unit square $\Omega = [0, 1]^2$:

$$\begin{cases} \min_{u, f} J(u, f) = \frac{1}{2} \|u(x, \mu) - \hat{u}(x, \mu)\|_{\mathcal{L}^2(\Omega)}^2 + \beta \|f(x, \mu)\|_{\mathcal{L}^2(\Omega)}^2, \\ \text{s.t. } -\operatorname{div}(\kappa^{ad}(x, \mu) \nabla u(x, \mu)) + \delta(x) \cdot \nabla u(x, \mu) = f(x, \mu), \text{ in } \Omega, \\ u(x, \mu) = 0, \text{ on } \partial\Omega, \end{cases} \quad (5.2)$$

where the desired state function $\hat{u}(x, \mu)$, diffusion coefficient $\kappa^{ad}(x, \mu)$ and advection coefficient $\delta(x) = [\delta_1(x), \delta_2(x)] \in \mathbb{R}^2$ are as follows.

$$\begin{cases} \hat{u}(x, \mu) = x_1 x_2 (1 - x_1)(1 - x_2) + \mu x_1^2 x_2^2 (1 - x_1)(1 - x_2), \\ \kappa^{ad}(x, \mu) = \kappa_1(x) + \mu(1 + x_1), \\ \delta_1(x) = 1 + x_1 + x_1^2, \\ \delta_2(x) = 1 + x_2 + x_2^2. \end{cases}$$

$\kappa_1(x)$ is the same high-contrast function in Figure 1.

Firstly, we use FEM on a 64×64 uniform fine grid to construct the FOM and then select a snapshot matrix to derive the ROM with $r = 3$, serving as the initial value for the algorithm.

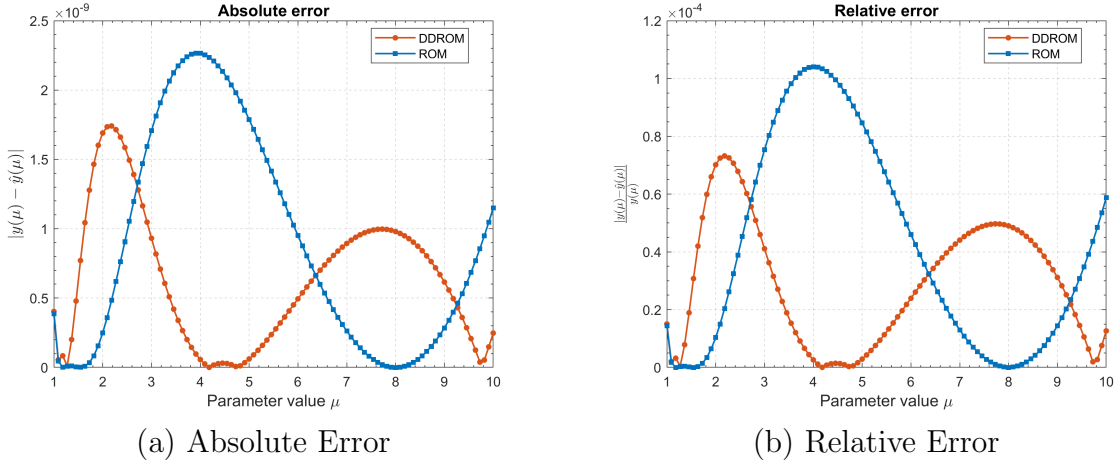


Figure 9: Error plots for the quantity of interest y with the finite element solution $y(\mu)$ as the reference, where $\hat{y}(\mu)$ is the interest of the reduced-order model.

Secondly, We construct the FOM on a uniform fine grid of 128×128 and a coarse grid of 8×8 by using the GMsFEM. Then the ROM with $r = 3$ is obtained by POD method as the initial value of the algorithm.

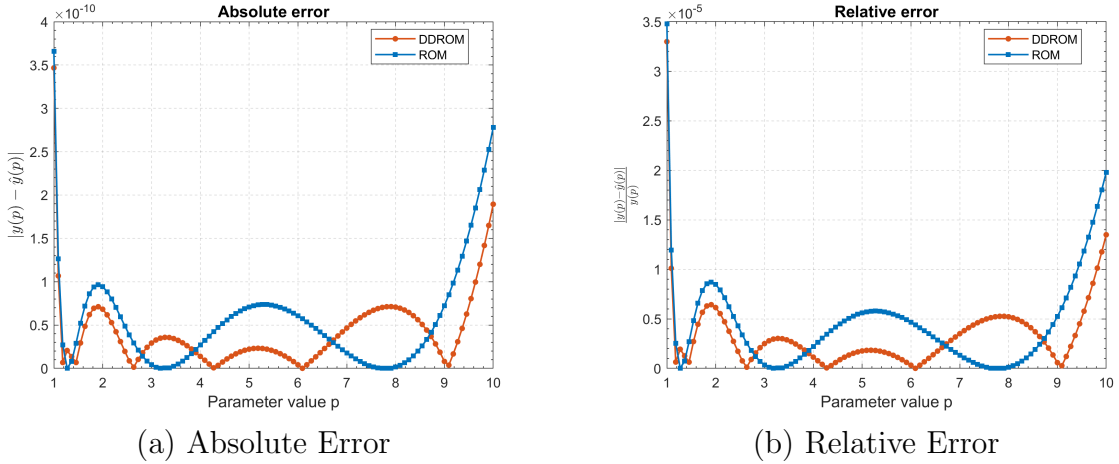


Figure 10: Error plots for the quantity of interest y .

The above error images reflect the effectiveness of the method to obtain DDROM, and then we give the images with the solutions at the center point of the sample $\bar{\mu}$.

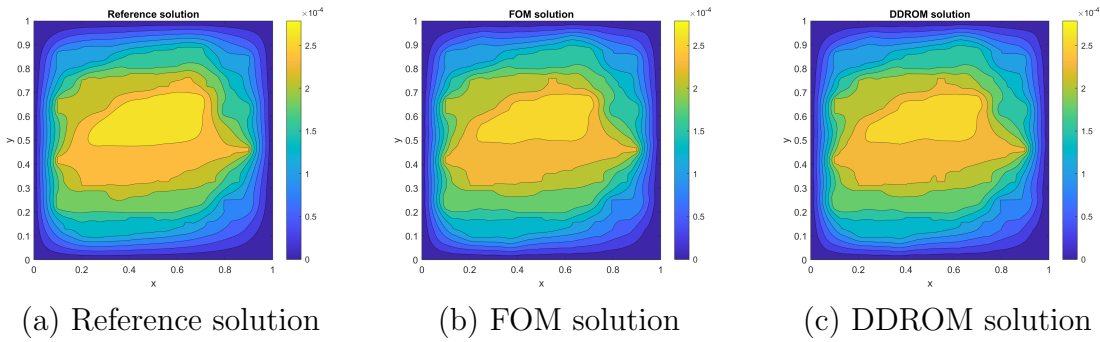


Figure 11: Images of solution U at $\bar{\mu}$.

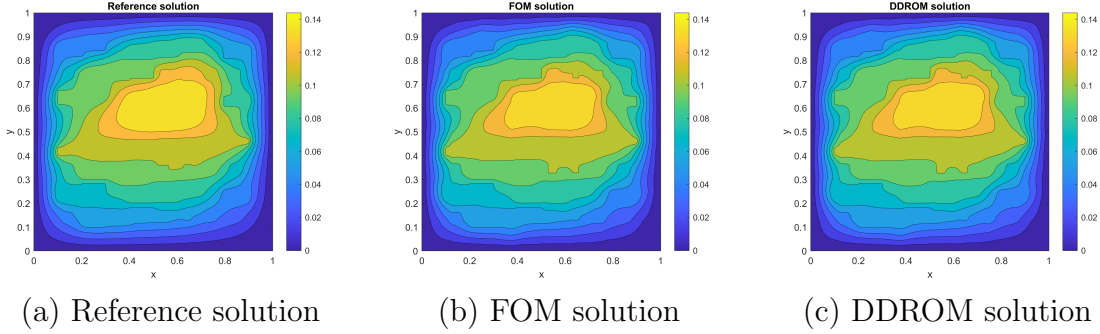


Figure 12: Images of solution F at $\bar{\mu}$.

6 Conclusion

References

- [1] J. Lions, *Optimal Control of Systems Governed By Partial Differential Equations*. New York: Springer, 1971.
- [2] R. Glowinski and J. Lions, *Exact and Approximate Controllability for Distributed Parameter Systems*. Cambridge, UK: Cambridge University Press, 1996.
- [3] T. Rees, H. Dollar, and A. Wathen, “Optimal solvers for pde-constrained optimization,” *SIAM J. Sci. Comput.*, vol. 32, no. 3, pp. 271–298, 2010.
- [4] M. Gunzburger, H. Lee, and J. Lee, “Error estimates of stochastic optimal neumann boundary control problems,” *SIAM J. Numer. Anal.*, vol. 49, pp. 1532–1552, 2011.
- [5] L. Hou, J. Lee, and H. Manouzi, “Finite element approximations of stochastic optimal control problems constrained by stochastic elliptic pdes,” *J. Math. Anal. Appl.*, vol. 384, pp. 87–103, 2011.
- [6] E. Rosseel and G. Wells, “Optimal control with stochastic pde constraints and uncertain controls,” *Comput. Methods Appl. Mech. Engrg.*, vol. 213, pp. 152–167, 2012.
- [7] H. Lee and J. Lee, “A stochastic galerkin method for stochastic control problems,” *Commun. Comput. Phys.*, vol. 14, pp. 77–106, 2013.
- [8] P. Chen, A. Quarteroni, and G. Rozza, “Stochastic optimal robin boundary control problems of advection-dominated elliptic equations,” *SIAM J. Numer. Anal.*, vol. 51, pp. 2700–2722, 2013.
- [9] S. S. Collis and M. Heinkenschloss, “Analysis of the streamline upwind/petrov galerkin method applied to the solution of optimal control problems,” Department of Computational and Applied Mathematics, Rice University, Houston, TX, Tech. Rep. TR02–01, 2002.